Master of Science Thesis

VT2013

Breathing interplay effects during Tomotherapy.
A 3D gel dosimetry study

Anna Ljusberg

Supervision

Sofie Ceberg, Joakim Medin,

Crister Ceberg and Lee Ambolt

Department of Medical Radiation Physics,
Clinical Sciences, Lund
Lund University

Table of contents

1. Abstract

Purpose: To evaluate if there are any breathing interplay effects during tomotherapy treatments and to see if the absorbed dose in a phantom corresponds to the planned absorbed dose.

Materials and methods: The detector used for this study is a normoxic polyacrylamide gel, nPAG. By irradiating two gel phantoms, one in motion and one stationary, two different absorbed dose distributions are obtained. By convolution of the static gel measurement with the motion pattern used for the dynamic gel measurement an absorbed dose distribution similar to the one in motion should be obtained. If there are differences between these, breathing interplay effects occur.

Results: The static gel measurements and the planned absorbed doses from the treatment planning system (TPS), agreed within 1,0 ± 1,0 % for the 95 % isodose volume. When motion was induced the 95 % isodose volume was under dosed due to dose smearing effects and the mean value of the difference between the two volumes were 5.5 ±3.2 %. For lower absorbed dose volumes, both under and over dosed volumes appeared in a spiral form. The spiral form could be explained by the breathing motion and the fast gantry rotation.

Conclusion: For the first time breathing interplay effects were shown for tomotherapy. Without motion of the tumour the TPS and measured absorbed dose agreed well. When motion was induced an under dosage of the target was found and also under and over dosed volumes forming a spiral in the low, <70-80 %, absorbed dose volume.

2. Popular scientific summary in swedish

I Sverige får 55 000 personer cancer varje år och 60 % utav dessa lever i mer än 10 år efter det att de fått sin diagnos. Detta tack vare den utveckling som skett inom diagnostisering och behandling. En utav de vanligaste behandlingssätten av cancer är strålbehandling, ca hälften av alla som drabbas får strålbehandling.

På strålbehandlingen vid Skånes universitetssjukhus kan man erbjuda behandling med tomoterapi. *Tomo* är grekiska och betyder skiva, behandlingen ges genom att skivsegment av kroppen bestrålas. En tomoapparat liknar en skiktröntgen, CT, till utseende och funktion. Precis som vid bildtagning med CT så placeras patienterna på en brits som åker in i en munkliknande öppning. Runt patienten roterar ett strålhuvud där joniserande strålning skapas. Den joniserande strålningen består av fotoner precis som röntgenstrålning och vanligt ljus. Enda skillnaden på fotonerna är att de har olika energi. Målet med strålbehandling är att kunna bestråla tumören så mycket som möjligt samtidigt som man håller den absorberande dosen (upptagen energi per kg) till den friska vävnaden så låg som möjligt eftersom fotonerna även skadar den friska vävnaden.

En fördel med tomoterapi är att man kan få välavgränsade områden där stråldosen är hög medan vävnaden runt omkring skonas från stråldos. Detta är möjligt på grund av att man kan bestråla tumören från 360° och i centimetertunna skivor. En nackdel med att behandla med tunna skivor är att om tumören är lång så fås en lång behandlingstid, vilket kan vara obekvämt för patienterna och kan leda till att patienterna rör på sig under behandling. En patientgrupp som gynnas av tomoterapi är de med riskorgan nära behandlingsområdet. Ett exempel är tumörer i huvudhals regionen där riskorgan så som spottkörtlar och ryggmärgen ofta ligger nära inpå tumören.

I detta examensarbete har geldosimetri använts för att undersöka kvalitén för behandling med tomoterapi. Experimenten har inte gjorts på riktiga tumörer i patienter. Istället har en volym motsvarande en tumör använts och bestrålningen är gjort i ett gelfantom. Dosimetri är ett uttryck som används för beräkning och mätning av hur mycket energi som tagits upp av kroppen vid bestrålning. I detta experiment har vatten och gelatin använts för att skapa en gel, i denna har sedan monomerer tillsatts. Vid bestrålning bildas polymerer utav monomererna. Med hjälp av magnetresonansbildtagning, MRI, kan man ta reda på hur stora polymererna har blivit under bestrålningen. MR-bildtagning beskriver väteprotonernas rörelse i vatten. Då det finns stora molekyler i vattnet så som polymerer så begränsas rörelsen hos väteprotonerna medan om det inte finns polymerer så kan väteprotonerna röra sig mer obegränsat. Detta leder till att MR-signalen blir olika beroende på storleken hos polymeren.

Med hjälp av geldosimetri kan man få en fördelning av den absorberade dosen motsvarande den som blir i kroppen vid behandling. Slutresultatet av denna undersökning är att dosfördelningen som levererats är nästan identisk med den som beräknats. För den volym som får 95 % av den levererade dosen är det en medelskillnad på 1,0 ± 1,0 %, förutom för tumörer i rörelse. Tumörer i lungområdet rör sig ofta med diafragman vid andning och eftersom bestrålning sker i tunna skivor finns en stor risk att tumören inte befinner sig där det är planerat, vilket gör att delar av den bestrålade volymen kan få för hög absorberad dos och andra för låg. I en jämförelse mellan en stillastående tumör och en i rörelse är det en medelskillnad på 5,5 ± 3,2 % för den volym som får 95 % av den absorberade dosen och 4,9 ± 5,2 % för den volym som får 50 % av den absorberade dosen. De volymer som fått för hög eller för låg absorberad dos bildar en spiral i lågdosområdet, vilket var intressant.

3. Introduction

Tomotherapy delivers intensity modulated radiation therapy, IMRT, which enables highly advanced treatment plans with homogenous absorbed dose coverage of the target with sharp dose gradients to spare surrounding healthy tissue. Helical tomotherapy consists of a linear accelerator mounted on a rotating gantry, the construction is similar to a CT although the energy is in the MV-range instead of kV and extra collimators and beam stopper are inserted [1-3].

During all kinds of radiation therapy patient motion is a concern since it can move the tumour outside the irradiated volume [4]. This will cause under or over dosed volumes which is an undesired effect, especially under dosage of the target or over dosage of organs at risk, OAR. Motion during radiation therapy is divided into two categories, intrafraction and interfraction motion. Interfraction motion is when the tumour moves between two different treatment sessions and intrafraction motion is when the tumour moves during a treatment session [5]. Tumours located in the abdomen often change location depending on the content of the stomach and intestine. This is an example of interfraction motion. Examples of intrafraction motion are movements due to the beating of the heart, coughing or breathing. For tumours in the thorax region breathing movement has the largest impact on the treatment [4, 6]. In conventional radiation therapy this is handled by creating a new volume including the clinical target volume, CTV, but also uncertainties in position and motion. There are two types of volumes that include these uncertainties, these are the internal target volume, ITV, and the planning target volume, PTV. The ITV includes uncertainties in positions within the body while the PTV also includes set-up deviations. For treatment planning the PTV is used and as a minimum the PTV has to be covered with the 95 % isodose volume of the absorbed dose that is prescribed.

The aim of this study is to evaluate the delivered absorbed dose in 3D compared with the planned absorbed dose by the Tomotherapy treatment planning system and also to see how simulated breathing motion affects the delivered dose. To do this gel dosimetry is used. The idea of using a gel that changes properties when irradiated was first suggested in the 1950's [7]. Since then, gel dosimetry has developed and is today a very useful tool for evaluating new equipment and treatment methods. The benefit of gel dosimetry is that it has high-resolution in three dimensions and that it is independent of the incident angle of the irradiation unlike many other detector systems [7]. Another advantage is that the gel is almost soft-tissue equivalent [8].

In decades a group of scientists in Malmö have used and developed the technique, and also applied it to IMRT- and VMAT-measurements [9-13]. To evaluate breathing interplay effects two gel phantoms are irradiated, one stationary and one in motion. If there is a difference between the two measurements that can not be explained by the simulated motion, breathing interplay effects have been found. Aside from the breathing interplay effect a comparison between the calculated dose distribution and measured dose distribution is done.

4. Theory

4.1 Tomotherapy

The theory of treating patients with a narrow fan shaped beam slice by slice was first suggested in the late 1980's by a group of scientists at the University of Wisconsin. However, the idea was put aside due to the fact that there might be gaps in absorbed dose between the delivered slices and it wasn't until the helical CT-systems was introduced that the idea came to life again and in 2001 the first patients were treated [14]. Since the concept was to treat the patient slice by slice, the greek word of slice was used to name the technique, hence the name tomotherapy. One of the leading scientists in developing the helical Tomotherapy system is Thomas Rockwell Mackie, who not only developed the technique, but also the treatment planning algorithm [2, 15].

Unlike most other linear accelerators used for cancer treatment tomotherapy doesn't have a flattening filter. Without the flattening filter the intensity of the beam is twice as high in the centre compared to the edges and the mean energy varies only as little as 5 % over the field, which is significantly lower than for units using flattening filter [1]. The radiation field is fan shaped with a maximum transverse width of 40 cm, at isocenter, and with a variable longitudinal width of approximately 1.0, 2.5 or 5.0 cm. With thin slices more conformal plans can be made compared with thick slices, but with the disadvantage that the treatment time will increase. A multi leaf collimator, MLC, can further modulate the field. For a tomotherapy unit the MLC consists of 64 leaves, 0.625 cm width at isocenter, that are either opened or closed and it takes about 20 ms for a leaf to move between the two settings [16].

Treatment plans for tomotherapy are calculated on CT-sets that have been imported into tomotherapy's own treatment planning system Tomotherapy Planning Station, TPS. The TPS uses an inverse dose calculation algorithm, that make use of iterative filtered back projection [15], where different PTV and OAR are associated with a certain dose. A minimum volume that has to be covered with a certain absorbed dose and a weight factor of how important this particular criterion is to fulfill is also recorded. For each gantry rotation there are 51 projections used for planning [16]. During one projection the MLC leaves can be opened for different times depending on how much absorbed dose is prescribed to a particular voxel. Before planning one has to decide what slice width that is to be used, what the pitch ratio is going to be and the maximum modulation factor. The modulation factor is defined as the ratio between the longest leaf opening time and the average opening time of all non-zero opening times and the pitch ratio is defined as the distance that the couch travels per gantry rotation divided by the treatment slice width [3].

The slice width is determined depending on the length of the target. For long targets a wide width is used to reduce the treatment time. A disadvantage of a wide slice thickness is that conformity in the craniocaudal direction is hard to achieve. Although this can be improved by reducing the pitch ratio instead of changing the width, although this also increases the treatment time. The pitch ratio should always be less than one to ensure overlapping between the slices. Another advantage of a low pitch ratio is that it's possible to achieve a higher absorbed dose per fraction. Since there is a maximal output per rotation the amount of absorbed dose is limited by this but by having a low pitch ratio the rotations overlap each other and build up the absorbed dose in that section.

The maximum modulation factor is often set between one and three and the value varies during the inverse treatment planning and it is not until the calculations

are done that the actual modulation factor is determined. For symmetrical targets close to the central axis a small modulation factor can be used [17].

The main advantage of tomotherapy is the many incident angles that enables homogenous dose distribution with sharp dose gradients [3]. To spare different OAR different angles can be defined where the radiation is blocked although conform plans can still be achieved. Another benefit is the ability to treat simultaneously integrated boosts, SIB [18]. Where different parts of the PTV can be prescribe different absorbed doses.

Tomotherapy's primary advantage is for patients with complex target volumes close to OAR [18]. Examples of these kinds of targets are different head and neck cancers that are close to the medulla and the parotid glands. It has been shown that with tomotherapy the mean absorbed dose to the parotid glands can be reduced and the unwanted side-effect of xerostomia can be minimized which is of great importance for patients [18, 19].

A distinction with tomotherapy compared to conventional treatments is that an increased number of monitor units, MUs, are needed, as compared to a non-wedged conformal plan [18]. That, together with the many angles of incidence enhance the volume of low absorbed doses. The effects of larger absorbed dose volumes are not entirely known. Although the large volume is needed to assure a high conformal absorbed dose in the PTV even though it increases the risk of evolving a secondary cancer. Another disfavour of the increased number of MUs are that it prolongs the total treatment time. A disadvantage of tomotherapy is that currently the field widths are fixed, which create unnecessary dose volumes in the craniocaudal direction. This has a considerable influence especially when the field width is long and there is an OAR located superior or inferior to the target. For field widths of 5 cm the radiation is activated when the first part of the target is in the field, which irradiate almost 5 cm extra of healthy tissue. To eliminate this problem Accuray has released TomoEDGE in their latest version. TomoEdge enables dynamic jaws that sweep over the target with a small opening at the beginning and end, and a maximal opening during the target. The main benefit of this is that the conformity at the edges of the target will improve significantly [20].

4.2 Dose smearing and breathing interplay effects

For tumours in the thorax region it is common that the tumour is moving in a longitudinal direction along with the diaphragm [6]. When treatment is delivered for a static conventional radiation field the risk of the tumour being outside the field is increased due to motion if the motion isn't considered in the PTV. A dose smearing effect is likely to occur which result in a lower achieved mean absorbed dose in the PTV and a larger volume of surrounding healthy tissue being irradiated [5]. This effect is always present for intrafraction motion but by using for example MLC-tracking, gating or expanding the PTV the effect of a lower absorbed dose in the target can be minimized. By expanding the PTV the reduced high absorbed dose volume is expanded to cover the tumour but this also increase the volume of healthy surrounding tissue being irradiated. Breathing interplay effects can also occur, if a multi leaf collimated radiation source with intensity modulation is used [5]. These effects are defined as the difference between planned and delivered absorbed dose that arise from a mismatch between the tumour and the MLC because of motion. In an extreme case parts of the tumour can be blocked by a MLC during a whole treatment session and other parts be irradiated during the whole session even if that wasn't planned. This can cause severe under- or over-dosed volumes resulting in cold and

hot spots of the target since the plan is based on a fixed tumour location. This occurs during every fraction and fortunately it has been shown that this effect will decrease with the number of fractions delivered [5, 21]. However, lung cancer is sometimes treated with stereotactic treatments with a high absorbed dose per fraction during only a few number of sessions [22]. During tomotherapy treatment it is not only the tumour and the MLC that is moving it is also the radiation source and couch, which can make the interplay effect more complex. Also important is that for tomotherapy the radiation source rotates around the patient in an average of 20 seconds compared to other rotational therapies were the radiation source rotates during one minute around the patient. To examine dose smearing effects and breathing interplay effects a detector with high resolution in 3D is needed since the distribution of under and over dosed volumes are hard to predict.

4.3 Gel dosimetry

To use radiation sensitive gel as a dosimeter was first suggested by Day and Stein during the 1950 [7]. Since then many different gels have been made and tested and in 1994 Maryansky et al manufactured a gel consisting of acrylamide (Aam), N,N'-methylene-bis-acrylamide (Bis), gelatine, water and nitrogen. This gel was commercially called BANG [23]. Aam and Bis are monomers, that when irradiated polymerizes. The gelatine is used as a matrix substance to ensure spatial resolution. To avoid oxygen in the gel nitrogen nitrogen is bubbled into the gel during fabrication. The reason for that is that oxygen prohibits the polymerization process of the monomers. Since '94 different compositions of the gel have been tested and the common name used for these types of gel dosimeters is polyacrylamide gel, PAG. In this study a normoxic PAG, nPAG, is used. The difference is that instead of nitrogen an oxygen scavenger is used to exclude oxygen from the gel.

When irradiated the water molecules in the gel undergoes radiolysis, which creates free radicals. The main products from this process are the hydrated electron (e^-_{aq}), the hydroxyl radical (OH•), and the hydrogen radical (H•). These have an unpaired valence electron that makes them very reactive. They react with monomers, Aam and Bis, and start a chain propagation of polymerization [7].

The free radicals are within nanometres from the incident radiation path, which implies that the polymers are created along the radiation path. The chain propagation is terminated when either two radicals recombine or disproportionate, that is when two free radicals react and create two non-radical end products[7].

There are two types of monomers in the gel, Aam and Bis. Aam forms long chains when polymerized, while Bis is used as a crosslinker that curls up the polymers.

If there is oxygen present in the gel the free radicals may react with it and form peroxide-radicals. This is an unwanted reaction since the peroxide-radicals will react with each other and recombine, which leads to termination. To prevent this nitrogen or other inert gases are bubbled into the gel during fabrication for PAG dosimeters and for nPAG dosimeters an oxygen scavenger is used.

Benefits of using nPAG instead of PAG are that the dose response of nPAG is less dependent of the temperature during irradiation and less sensitive to dose-rate fluctuations than PAG dosimeters. However both gels are sensitive to changes in temperature during MRI-read out [8]. To minimize the effect of this the phantom should be stored for several hours in the MR-room to establish thermal equilibrium before read out. The temperature during the cooling down of the gel also affects the quality of the gel. This is assumed to be due to the fact that the gel and the oxygen

scavenger interact with each other differently depending on temperature[24]. If different gel phantoms are to be compared one should use phantoms of the same size to achieve similar cool down rates. One should also be careful using large phantoms since the temperature gradient in the gel will be steeper.

4.4 MRI read out

There are several techniques for read out of gel dosimeters, for example optical CT, x-ray CT and ultrasound [7]. In this study MRI is used for read out. The contrast in the MR-image depends on the characteristics of the gel. The hydrogen protons in water are less mobile when surrounded by polymers than monomers. This implies a high spin-spin relaxation rate, R_2, in a polymer rich environment since the protons interact with each other and create a static inhomogeneous magnetic field. For hydrogen protons, surrounded by monomers, which are able to move easier the spin-spin relaxation rate will be low. This is due to that the fast changes in the local magnetic field are averaged out and there is no residual magnetic field inhomogenity. The spin-spin relaxation rate is inversely proportional to T_2. T_2-weighted images are often used clinically and from these R_2-maps can be calculated. In a T_2-weighted image water will have a higher signal than monomers, which will have a higher signal than polymers. The signal, S, in a T_2-weighted spin-echo sequence can be described by

$$S = S_0 \cdot e^{-\frac{TE}{T_2}} + C = S_0 \cdot e^{-R_2 \cdot TE} + C$$

Equation 1: The MR-signal.

where TE is the echo-time and C is a constant. The advantage of using a spin-echo sequence is that local magnetic inhomogeneities, T_2*-effects, doesn't influence the read-out. To improve the signal-to-noise ratio, SNR, a multi spin-echo sequence can be used. Then several pictures are collected with an echo time of multiples of TE_1. R_2 can be extracted for every pixel by fitting an exponential decay curve to the signal intensity in a certain pixel in every image. Since R_2 depends on the signal and the signal depends on the characteristics of the gel the relaxation rate will increase with the size of the polymer. The polymer size, as mentioned earlier, depends on the absorbed dose in that volume. In conclusion R_2 –maps can be converted to relative absorbed dose distributions. If an absolute measurement of the dose is executed, for example with an ionising chamber detector, an absolute dose distribution can be obtained otherwise it is relative to a chosen normalisation point. The normalisation point should be placed somewhere in the middle of the PTV were there are no sharp dose gradients.

5. Material and methods

Tomotherapy planning and delivery was performed at Skåne University Hospital, SUS, in Lund while gel preparing and MRI read out was carried out at SUS Malmö. As a first experiment it was investigated if gel dosimetry was applicable on tomotherapy. The second experiment had two purposes, the first one was to compare delivered absorbed dose with the planned absorbed dose for a small target and the second purpose was to investigate if breathing interplay effects was present.

5.1 Gel preparation

The nPAG used in this study consists of 3 % w/w Acrylamide (electrophoresis grade ≥99 %, powder, Sigma Aldrich), 3 % w/w N',N'-methylenebisacrylamide (electrophoresis grade ≥ 98%, powder, Sigma Aldrich), 10 mM tetrakis(hydroxymethyl)phosphonium chloride (techn. 80 % in water, Sigma Aldrich), 5 % w/w gelatine (from swine, Sigma Aldrich) and 89 % ultra-pure deionized water (resistivity > 18.2 MΩcm). This recipe is based on studies performed by earlier groups with similar experiments. This type of gel has also been shown to be suitable for dynamic studies [11]. The preparation of the gel is done in a fume cupboard. First the water is measured and poured into a large container and before adding the gelatine a magnetic stir bar is put in the container. When the gelatine is mixed with the water the solution is heated to 45 °C and Aam is added. Since Aam is neurotoxic one should be careful when handling it and use protection gloves and mask. To minimize polymerization of the monomer before irradiation the gel should be prepared, if possible, and stored in darkness. When the Aam is dissolved, which takes about 20 min, the Bis is added and it takes another 20 min for it to dissolve. After that, the temperature is lowered to 37 °C and the oxygen scavenger, THP, is added. Some minutes after the THP has been added the speed of the magnetic stir bar is lowered, which enables air bubbles to rise to the surface. The mixture is then poured into phantom bottles and small vials. The vials are used to verify that there is a linear relation between the delivered number of monitors units and the absorbed dose response. The bottles are then set in the dark to rest for 24 hours.
The glass bottles used contained 1.1 l and for the first study 2 bottles were used, one being irradiated and one used to measure background irradiation. For the second experiment three bottles were used, one for background measurement, one for a static measurement of a small target and the last bottle were used for a dynamic measurement. The number of small vials, containing 15 ml, was 8 and 9 respectively.

5.2 Treatment planning

The treatment plans were calculated with TomoTherapy PlanningStation version 4.2.0.87 (TomoTherapy Incorportated, Madison, Winsconsin, USA). The phantoms were CT-scanned when the gel had been stored for about 24 hours. It was not only the phantoms that were to be irradiated that were CT scanned but also the phantoms used for background measurements. CT-scans need to be taken to enable dose planning but when comparing the absorbed dose between the phantom and TPS the contribution of absorbed dose from the CT-scan and also background irradiation needs to be excluded. This exclusion is done by doing a background measurement with a similar phantom that is treated in the same way as the real phantom, in storage and CT-scanning but with the exception of being irradiated with the tomotherapy treatment unit.

The CT-images were scanned using a Siemens CT- scanner and for the first experiment a slice thickness of 3 mm was used and for the second experiment a slice thickness of 5 mm were used. The phantom was positioned with cross-lasers and markers were drawn on, to enable the same set-up during radiation.

For the first experiment the CT-images were imported to the TPS in the same way patient images are handled. The PTV was constructed as a cylinder, with a height and diameter of ~6 cm, and assigned an absorbed dose of 2 Gy. For the second study the CT-set was read in as a phantom, which allows creation of DQA-plans. The DQA-plan consists of the same parameters as the patient plan but the dose distribution has been recalculated on a new CT-set belonging to a homogenous phantom. Since the human body is inhomogeneous and every patient is different it is not possible to measure in that geometry and that is why a homogenous phantom is used. If the planed absorbed dose distribution is not recalculated then there will be a difference between measured and calculated absorbed dose since the phantom doesn't reflect the electron density in the patient. The DQA-plan makes it possible to measure the delivered absorbed dose to the phantom and compare it with the calculated absorbed dose for that phantom. For this experiment a patient plan was used and recalculated on the phantom. Treatment plan parameters (Table 1) are either chosen or a result of the iteration process.

To examine breathing interplay effects the same treatment plan was delivered both to a stationary phantom and to a phantom in motion.

Table 1: Parameters for the treatment plans.

Parameter	First experiment	Second experiment
Gy/fraction	2	3
Field width [cm]	2.5	2.5
Planning modulation factor	1.194	1.408
Pitch ratio	0.287	0.215
Planned field width [cm]	4.7	3.2
Couch travel [cm]	9.2	5.6
Couch speed [cm/s]	0.05979	0.04479
Expected delivery [Mu]	2 098	1 688
Duration [s]	153.2	125.2

5.3 Irradiation

5.3.1 Linearity test

The small vials used for the linearity test were irradiated with a conventional linear accelerator. For the first study one vial was stored in a cupboard during the whole time, one was with the other vials but not irradiated and the other were irradiated with 50, 100, 150, 200, 300 and 400 MU respectively. For the second experiment one vial was not irradiated, but stored with the others at all times, and the others were irradiated with 100, 150, 200, 250, 300, 350, 400 and 500 MU respectively. The small vials were placed in a cubic water phantom that was placed at SSD=100 cm and irradiated with a field of 20 x 20 cm^2.

5.3.2 Experiment 1

The irradiation was performed 24 hours after gel fabrication with the TomoThearapy HD system (TomoTherapy Incorporated, Madison, Winsconsin, USA). The gel was

positioned with the aid of cross lasers and MVCT images were taken with the tomotherapy unit to be used for set up. MVCT images were also taken on the background phantom.

5.3.3 Experiment 2

For examination of breathing interplay effects a robot, HexaMotion (ScandiDos, Uppsala, Sweden), was used to move the phantom. The HexaMotion was modified and instead of holding the Delta4 detector, which it is constructed for, a plate of PMMA was mounted where the gel bottles could be placed. It was programmed to move in a sinusoidal pattern with a peak-to-valley distance of 20 mm over a period of 6 seconds. This motion pattern is within the normal range of lung tumour motion according to a study by Y. Seppenwoolde et al[4]. The movement was in the longitudinal direction, along with the diaphragm, perpendicular to the irradiation plane. As mentioned above there was a couch movement of 5.6 cm during the treatment and the duration of the treatment was 125.2 s. This means that there was a motion of the target with 0.45 mm/s due to couch motion. This is relatively small compared with the motion induced by the HexaMotion of 6.7 mm/s. The treatment was delivered in a helical way and one rotation for the radiation source took 12 s. If the couch movement is neglected the longitudinal movement per angular unit is

$$\frac{20/3}{2\pi/12}\text{mm/rad} = \frac{40}{\pi}\text{mm/rad}.$$

Equation 2: Movement per angular unit for induced motion.

If no motion is induced the movement per angular unit is

$$\frac{56/125.2}{2\pi/12}\text{mm/rad} = \frac{2.7}{\pi}\text{mm/rad}.$$

Equation 3: Movement per angular unit due to couch motion and gantry rotation.

Thus the induced motion changes the movement per angular unit with a factor of almost 15 and this will cause a mismatch between the planned absorbed dose and the actual received absorbed dose and could cause a breathing interplay effect. If a breathing interplay effect is visible it is likely to form a helical spiral with a rise of $40/\pi$ mm/rad since that is the movement that is induced.

5.4 MRI read out

After irradiation the polymerization begins and MRI read out was not performed until the next day when termination of the polymerization had occurred. A minimum waiting time between irradiation and read out is 10 h [7]. The MR-images were acquired using a multispin-echo on a 1.5 T MRI-unit (Siemens Symphony, Siemens Medical Solutions, Germany). Parameters used for image acquiring (Table 2) are chosen for an optimal measurement without to much noise in the picture but with an acceptable acquisition time. To minimize interference between nearby slices the slices were acquired in two parts were the parts were shifted one slice thickness and only every other slice was collected.

The number of slices depends on the size of the irradiated volume. For the cylinder and the dynamic small target 32 slices were collected and for the static small target 30 slices were used. For the background bottles 6 and 4 slices were used for the

cylinder experiment and the small target experiment respectively.

Table 2: Parameters used for collecting MR-images. Values in brackets are used for the background bottle.

Parameter	Value
Time between echoes, TE	25 ms
Time of repetition, TR	6520 (4000 ms)
Field of view, FOV	256 x 256 mm^2
Slice thickness	3 mm
Pixel size	1 x 1 mm^2

5.5 Data analysis

With the use of an in-house developed programme the MR-data were converted to R_2-distributions. This conversion was done with a fit of an exponential decay curve (Equation 1) to the signal in each pixel with different TE. The curve was optimized using the Levenberg–Marquardt optimizing algorithm. The three first echoes were excluded from the calculation due to the uncertainty in signal intensity due to eddy currents induced in the coils. The constant C is optimized for the background bottle and then applied to all other optimizations.

For comparison of the data MATLAB (R2012b (8.0.783)) was used. The R_2-distribution and the treatment planning data were resampled to 1 x 1 x 1 mm^3. To attain a relative absorbed dose distribution a background subtraction was performed for the R_2-distribution with the data achieved from the unirradiated phantoms. The data was smoothed by convolution with a kernel consisting of 3 x 3 x 3 voxels. For the first experiment the normalization was done to a volume of 125 voxels located in the middle of the cylinder. For the second experiment the absorbed dose volume was normalized to only 1 voxel in the center of the target where there was no sharp dose gradient. The different data-sets were matched using profiles of the data. The static and dynamic gels were match according to the edges of the phantom bottles and the TPS was matched with profiles over the target.

As mentioned earlier the breathing interplay effect is defined as the difference in absorbed dose due the induced motion. To investigate breathing interplay effects the absorbed dose distribution from the static gel measurement was convolved with the motion function of the HexaMotion. The obtained result is how the measured dose distribution should be if no breathing interplay effect is present when motion is induced. The difference, if there is one, between the convolved measurement and the dynamic measurement is seen as the breathing interplay effect.

To evaluate the relative absorbed dose the volume within the 95 % isodose and 50 % isodose surfaces were compared between the gel and TPS. Histograms are displayed to show the distribution of the differences of the measured and calculated absorbed doses.

6. Results

6.1 Linearity test

The test with the vials confirmed the linearity of the gel. The result of the linear regression for the gel used during the first experiment was

$$R_2 = 1.3 \cdot 10^{-3} \cdot \mathrm{Mu} + 0.94,$$

Equation 4: Linear relation for the first gel batch.

with a coefficient of determination, R^2, of 0.999. For the regression the unirradiated vial that was together with the other at all times was used for 0 MU. The difference between the vial stored in a cupboard and the unirradiated vial was 0.04 s^{-1}. The result of the regression for the second gel was

$$R_2 = 1.3 \cdot 10^{-3} \cdot \mathrm{Mu} + 0.95,$$

Equation 5: Linear relation for the second gel batch.

with R^2 as 0.998. From the calculated R_2-value an estimation of a linear curve is done (Figure 1).

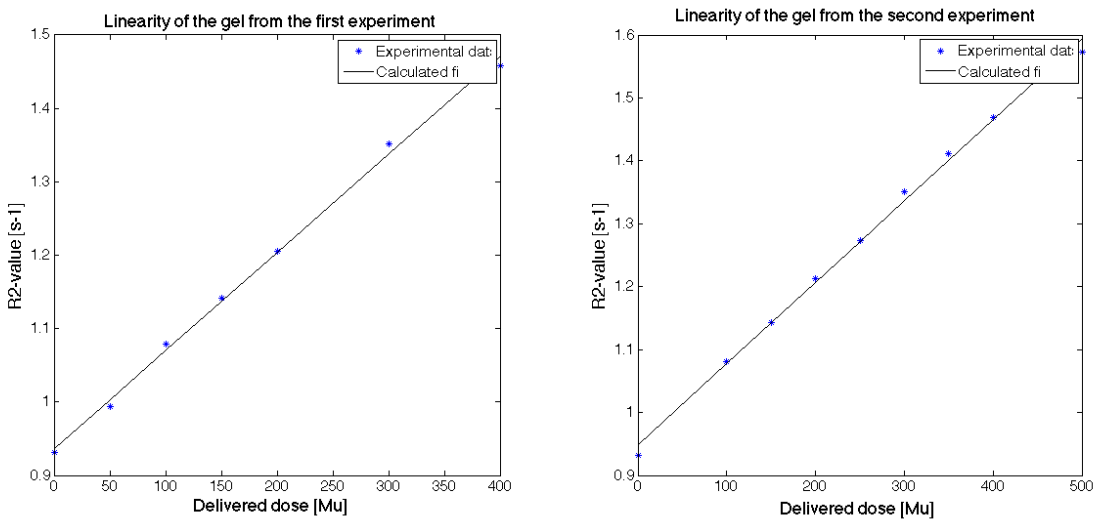

Figure 1: Linearity control of the first (left figure) and second (right picture) gel batch.

6.2 Experiment 1

The isodose surface corresponding to 95 % of the absorbed dose, VOI_{95}, is calculated together with the 95 and 50 % isodose lines from two slices (Figure 2), one being located in the middle and one closer to the end of the cylinder. The mean value in VOI_{95} and VOI_{50} is 99.7 ± 1.8 % and 79.5 ± 17.8 % for the gel and 99.4 ±1.2 % and 79.0 ±18.3 % for the TPS. Voxel-by-voxel subtraction between the TPS and the gel measurement, with voxels corresponding to the volumes limited by the 95 and 50 % isodose surfaces in the gel, resulted in a mean deviation of -0.5 ± 1.5 % and -1.4 ± 2.5 % respectively. The distribution of the differences from voxel-by-voxel subtraction is plotted in a histogram (Figure 3**),** where the x-axis in the histogram is the difference

of absorbed dose in percent between two voxels and the y-axis describes how many voxels in percent of the whole volume that has this difference.

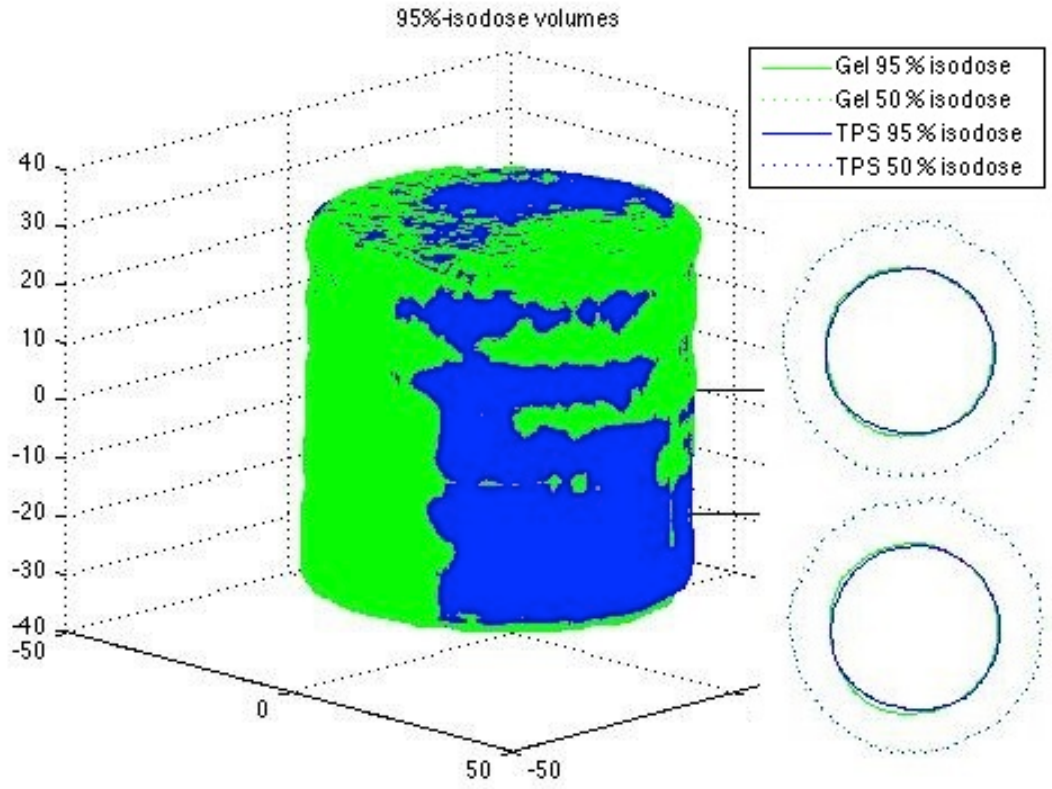

Figure 2: 95 % isodose volumes of the gel (green) and TPS (blue). In the figure there is also crossections with 95 % and 50 % isodose levels. The black line gives an indication of where the crossection slices are located.

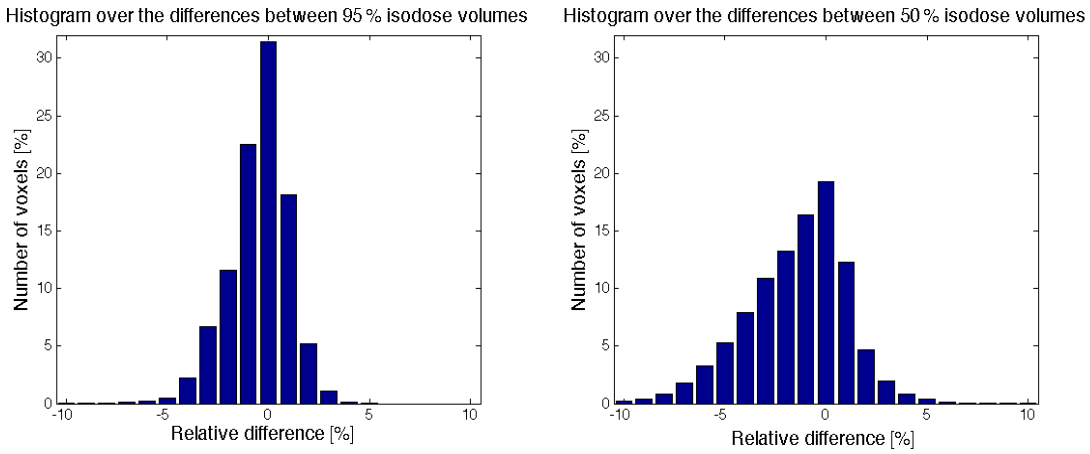

Figure 3: Distribution of voxel by voxel subtraction between the gel and TPS for 95 % isodose volume to the left and 50 % isodose volume to the right. The volumes are 188 cm^3 and 543 cm^3 respectively.

6.3 Experiment 2

An overlay of the 95 % isodose surfaces from the second experiment (left) and an overlay of the 50 % isodose surfaces (right) are displayed for the different measurements (Figure 5). At the top the TPS and the static gel measurement are displayed, in the middle the static and dynamic gel measurements are shown and at the bottom the dynamic and convolved static gels are demonstrated. The distribution of the differences between the volumes were calculated and displayed in a histogram (Figure 4). The voxels used for the subtraction are defined by the volume of the static gel for comparisons between the static gel and the TPS and the static gel and the dynamic gel. For comparisons between the dynamic gel and the convolved static gel, the volume of the dynamic gel is used.

The mean values and standard deviations of the differences between the volumes were calculated (Table 3).

Table 3: The mean value and standard deviation of the differences between volumes.

		Mean [%]	1 standard deviation [%]
95 % isodose volume	static gel - TPS	1.0	1.0
	static gel- dynamic gel	5.5	3.2
	dynamic gel- convolved static gel	-0.5	2.2
50 % isodose volume	static gel - TPS	2.5	1.4
	static gel- dynamic gel	4.9	5.2
	dynamic gel- convolved static gel	-0.02	4.6

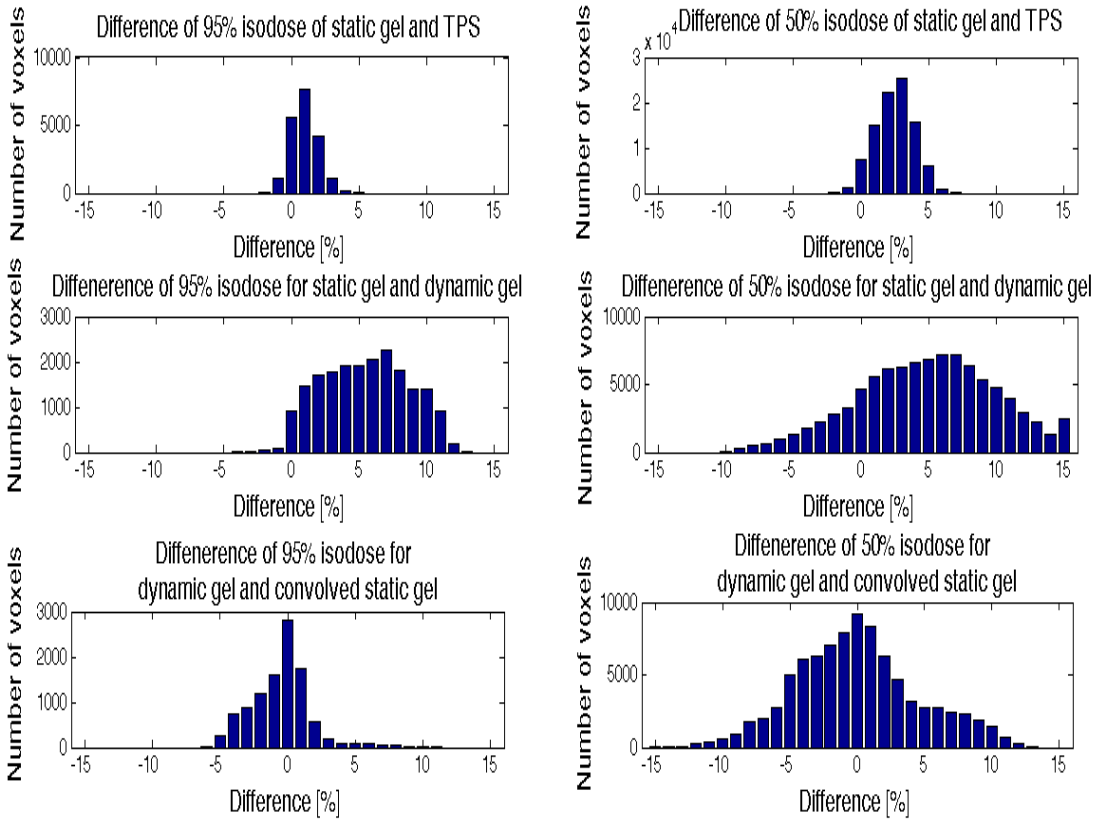

Figure 4: Histograms over the differences between the volumes displayed in Figure 5. Note the different scales on the y-axis.

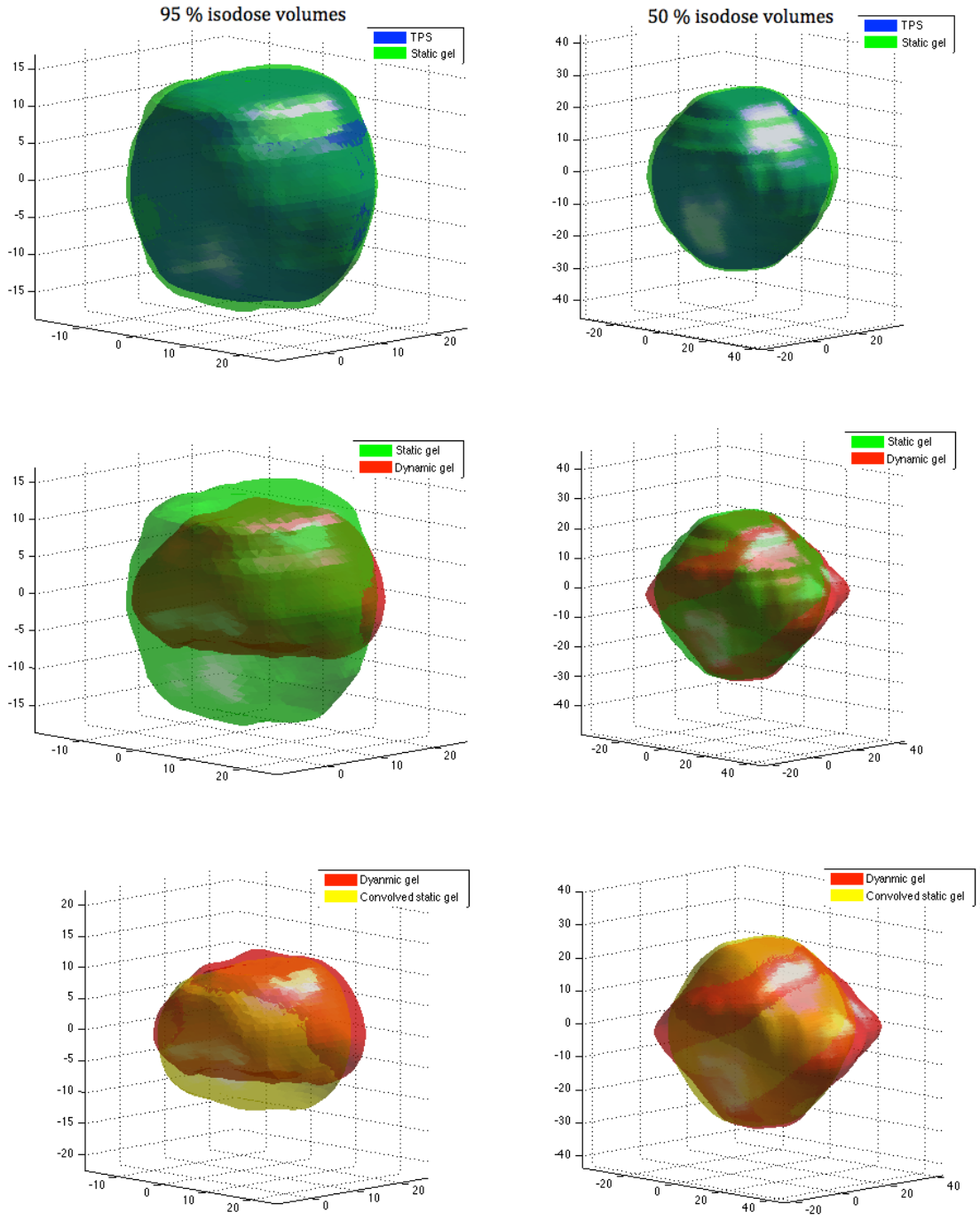

Figure 5: The 95 % isodose surfaces (left column) and the 50 % isodose surfaces (right column). At the top the static gel and TPS are seen, in the middle the static gel and dynamic gel are shown and at the bottom the dynamic gel is displayed together with the convolved static gel.

A subtraction between the dynamic gel measurements and the convolved static gel was performed. The surface of voxels with a difference of 5 % is displayed (Figure 6).

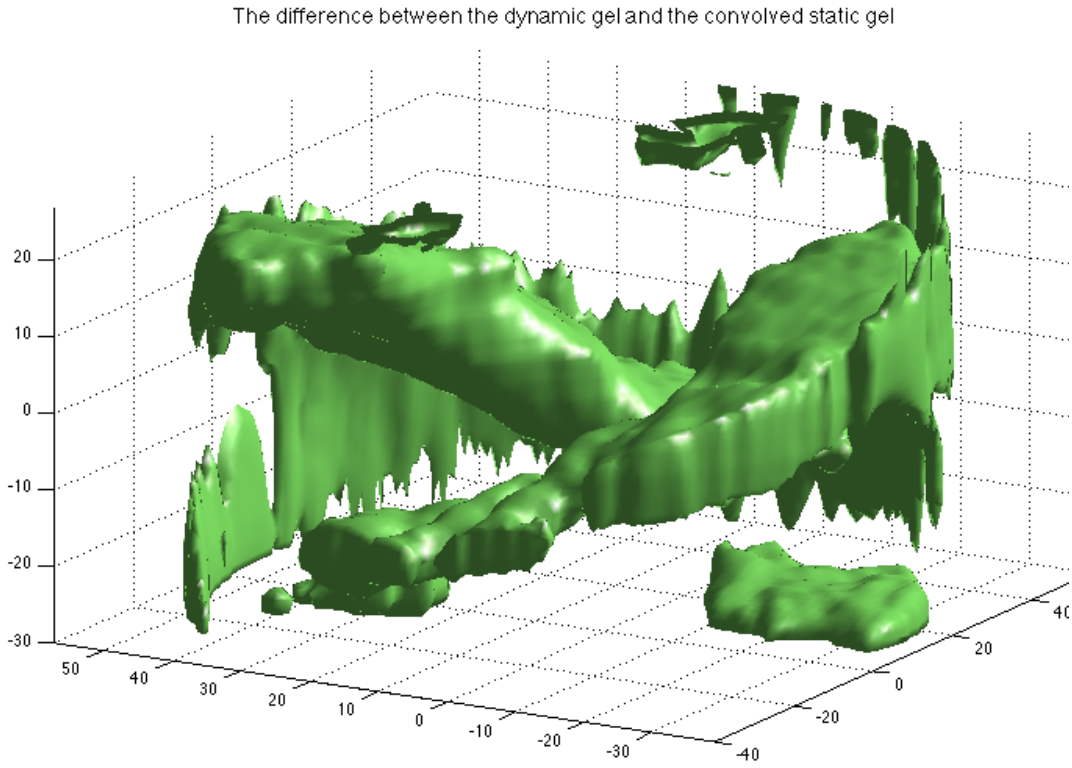

Figure 6: Difference of 5 % between dynamic gel and convolved static gel. Some parts of the phantom wall are also seen.

7. Discussion

Differences due to uncertainties in set-up of the phantom have been minimized by matching the volumes manually with guidance from profiles and phantom bottle edges. No rotation of the data has been performed. When performing a translation one can minimize or eliminate differences that are interpreted as a set-up deviation but could have other origins for example breathing interplay effects. For a better result one should use a phantom holder that positions the phantoms exactly the same during radiation and read out, although since laser and MVCT images are used the size of this error is only a few mm maximum.

All MRI-data was acquired in two segments with 3 mm slice thickness sampled with 6 mm in between. The two parts are separated by 3 mm and when combined slices are obtained every 3 mm. For the static gel the separation between the two segments where only 2.6 mm, which result in uneven distribution of the slices but since the data is assumed to be linear with absorbed dose and was resampled to 1 x 1 x 1 mm^3 the effect on the results is assumed to be negligible.

7.1 Linearity test

To assure that the compounds of the gel are in the right proportion and that they have been dissolved properly, a linearity test was performed. If the response of the gel is not linear no relative dosimetry can be executed. The gel had a strong linear relation with a coefficient of determination of 0.999 and 0.998 for the first and second batches of gel, respectively, and especially in the area between one to three Gy, which is of interest in these studies. Except having the right proportions of the gel other factors also affect the read out, for example cooling rate and size of the phantom. One should use a phantom that is large enough to enclose the target and also some of the lower isodose volumes. Due to oxygen effects data sampled close to the phantom wall should be ignored since the oxygen concentration can be higher here and as mentioned earlier oxygen will terminate the chain propagation quickly and lead to a non linear relationship with absorbed dose. To be able to compare two different measurements with each other as in the case for breathing interplay effects one should use the same sized phantoms since the cooling rate depends on the size of the phantom.

7.2 Experiment 1

The results from the cylindrical target shows good agreement of the absorbed dose measured with gel compared with the planned dose distribution. The mean of differences were small only -0.5 ± 1.5 % and -1.4 ± 2.5 % for VOI_{95} and VOI_{50} and that indicates that gel dosimetry is applicable on the tomotherapy unit. Desiring would have been a mean value of zero. One reason for not being zero can be the manual matching that has been done between the volumes and as seen in Figure 2 there are also differences for the voxels at the edges of the isodose volumes. The aim of this experiment was to use a simple target without motion to investigate the feasibility of using gel dosimetry for tomotherapy. If there would have been large differences between the planed and measured dose distribution it might not have been possible for a more complex target with motion. It has been shown earlier that gel dosimetry is applicable for IMRT- and VMAT-measurements but there are some differences between these treatments and tomotherapy such as the narrow field width, collimator scatter, stability of output and gantry rotation speed. This first experiment was also used for practice of all the different moments included such as gel fabrication, phantom positioning and MRI-read out.

7.3 Experiment 2

The 95 % and 50 % isodose surface of the static gel and TPS shows good agreement in size and location (Figure 5). The gel seems to be somewhat bigger in size and that is also confirmed by the positive mean value of the differences.

The 95 % isodose surface of the dynamic gel is smaller than the static gel, which is logical since the target edges has been outside the beam due to the simulated breathing motion. This dose smearing effect can be minimized by extending the PTV, so it includes the movements. The dose smearing effect does decrease the 95 % isodose surface but the extent of the 50 % isodose surface is comparable with that of the static gel. The mean value of the differences is in this case higher, which is explained by the difference in volume at the edges. The matching of the volumes in the craniocaudal direction has been made by using longitudinal dose profiles over the target. The matching of the dynamic gel has been done for 50 % isodose where they match well in size and location, while at the 95 % isodose level there is a slight mismatch. The mismatch is due to the dose smearing and interplay effects, caused by the simulated breathing motion, which have affected the dose distribution in an uneven way and the lower parts of the target has been under dosed.

The mean of the differences is very small in most cases except for the dynamic gel measurement compared with the static gel measurement where there is a dose smearing effect. The effect of the dose smearing is eliminated when the static gel measurement is convolved with the motion pattern, and there is only a small difference left between the convolved gel and dynamic gel measurement. This is indicated by the mean value, which is almost zero, albeit with a large standard deviation. A large standard deviation indicates that larger differences exist between the volumes. For the volume within 50 % isodose surface the standard deviation of the difference between the dynamic gel measurement and the convolved static gel is large, 4.6 %, and for the dynamic gel compared with the static gel measurement it is 5.2 %. In other words there are dose volumes that differ several percent and as seen in the histogram (Figure 4) there are differences up to ±10 %. Unfortunately a standard deviation or histogram does not include information of where these differences occur but since gel dosimetry has a spatial resolution in 3D the volumes can be studied, and these differences form a spiral (Figure 6). When comparing isodose volumes for a high absorbed dose these effects aren't visible but they appear in the lower absorbed dose volumes (<70-80%). The spiral outline is similar to the helical way the radiation is delivered but a quarter of a rotation in the figure corresponds to about 20 mm while the couch movement is only 5 mm for one rotation. Although the movement of 20 mm for a quarter of a loop corresponds well with the motion induced by the HexaMotion (Equation 2). With this experiment, when introducing one type of simulated breathing movement, under and over dosed volumes form a spiral that has a rise corresponding to the movement of the target per angular unit. This breathing interplay effect has only been shown for a certain field width but it can be assumed that the breathing effects will be worse with a smaller slice width since the target then will be outside the field even more.

8. Conclusion

Breathing interplay effects were observed during tomotherapy treatment when simulated breathing motion was induced to 3D polymer gel measurement. At the PTV and volumes with high absorbed dose a dose smearing effect was visible and for regions with lower absorbed dose over- and under-dosed volumes appeared in a spiral form. This could only be demonstrated due to 3D measurements with high spatial resolution. Gel dosimetry is presently a time consuming method and is not suitable in its current form for every day clinical work but it is a good tool for investigation of new equipment and treatment techniques as demonstrated in this thesis.

The conclusion of this thesis is that breathing interplay and dose smearing effects can appear during in tomotherapy when motion is induced. The breathing interplay effect affect the low absorbed dose volumes (<80%) and form under and over dosed volumes. Although the mean value is still close to zero and an over dosage in the 50 % isodose level is not as radical as if it were in the target volume. Important though is to be considerate before referring a lung cancer patient to tomotherapy since the dose smearing effect will decrease the absorbed dose in the target if the motion is not included in the PTV. For this study with the plan parameters and motion used the decrease was 5.5 ± 3.2 % for the volume enclosed by the 95 % isodose surface and simulated breathing interplay effects was shown for the first time for tomotherapy.

9. Acknowledgement

Thank you all my supervisors in guiding and helping me in your different specialities: Joakim and Lee with your tomotherapy knowledge, Crister with your MATLAB skills and Sofie, who to me is the expert in gel dosimetry. I would also like to thank Fredrik Nordström for his R_2-calculation programme, which was very useful. And thank you Mattias Jönsson for helping me with the HexaMotion.

10. References

1. Jeraj, R., et al., *Radiation characteristics of helical tomotherapy*. Medical Physics, 2004. **31**(2): p. 396-404.
2. Mackie, T.R., et al., *Tomotherapy: a new concept for the delivery of dynamic conformal radiotherapy*. Medical Physics, 1993. **20**(6): p. 1709-1719.
3. Piotrowski, T., et al., *Tomotherapy - a different way of dose delivery in radiotherapy*. Wspolczesne Onkologia-Contemporary Oncology, 2012. **16**(1): p. 16-25.
4. Seppenwoolde, Y., et al., *Precise and real-time measurement of 3D tumor motion in lung due to breathing and heartbeat, measured during radiotherapy*. International Journal of Radiation Oncology, Biology, Physics, 2002. **53**(4): p. 822-834.
5. Thomas, B., B.J. Steve, and R. Eike, *Effects of motion on the total dose distribution*. Seminars in Radiation Oncology, 2004. **14**(1): p. 41-51.
6. Yu, Z.H., et al., *Organ motion in lung cancer: A comparison of tumor motion characteristics between early stage and locally advanced stage lung cancers*. Radiotherapy and Oncology, 2012. **104**(1): p. 33-38.
7. Baldock, C., et al., *Polymer gel dosimetry*. Physics in Medicine and Biology, 2010. **55**(5): p. R1.
8. De Deene, Y., et al., *The fundamental radiation properties of normoxic polymer gel dosimeters: a comparison between a methacrylic acid based gel and acrylamide based gels*. Physics In Medicine And Biology, 2006. **51**(3): p. 653-673.
9. Ceberg, S., *3D verification of dynamic and breathing adapted radiotherapy using polymer gel dosimetry* Malmö, Skåne University Hospital, Lund University, 2010.
10. Ceberg, S., et al., *RapidArc treatment verification in 3D using polymer gel dosimetry and Monte Carlo simulation*. Physics in Medicine and Biology, 2010. **55**(17): p. 4885-4898.
11. Ceberg, S., et al., *Verification of dynamic radiotherapy: the potential for 3D dosimetry under respiratory-like motion using polymer gel*. Physics in Medicine and Biology, 2008. **53**(20): p. N387-N396.
12. Gustavsson, H., et al., *MAGIC-type polymer gel for three-dimensional dosimetry: Intensity-modulated radiation therapy verification*. Medical Physics, 2003. **30**(6): p. 1264-1271.
13. Karlsson, A., *Characterization and clinical application of normoxic polymer gel in radiation therapy dosimetry* Phd, Thesis. Malmö : Medical Radiation Physics, Malmö University Hospital, Lund University, 2007.
14. Mackie, T.R., et al., *Tomotherapy*. Seminars in Radiation Oncology, 1999. **9**(1): p. 108-117.
15. Holmes, T.W., T.R. Mackie, and P. Reckwerdt, *An Iterative Filtered Backprojection Inverse Treatment Planning Algorithm for Tomotherapy*. Internation Journal of Radiation Oncology, Biology, Physics, 1995. **32**(4): p. 1215-1225.
16. Langen, K.M., et al., *QA for helical tomotherapy: Report of the AAPM Task Group 148*. Medical Physics, 2010. **37**(9): p. 4817-4853.

17. Yartsev, S., T. Kron, and J.V. Dyk, *Tomotherapy as a tool in image-guided radiation therapy (IGRT): theoretical and technological aspects*. Biomedical Imaging and Intervention Journal, 2007. **3**(1): p. e16.
18. Wiezorek, T., et al., *Rotational IMRT techniques compared to fixed gantry IMRT and Tomotherapy: multi-institutional planning study for head-and-neck cases*. Radiation Oncology, 2011. **6**(1): p. 20.
19. Voordeckers, M., et al., *Parotid gland sparing with helical tomotherapy in head-and-neck cancer*. International Journal Of Radiation Oncology, Biology, Physics, 2012. **84**(2): p. 443-448.
20. *Accuray Launches New TomoTherapy® H™ Series Featuring TomoEDGE™* , in *MA-Accuray-TomoEDGE*2012: PR Newswire US, 10/28/2012.
21. Bortfeld, T., et al., *Effects of intra-fraction motion on IMRT dose delivery: statistical analysis and simulation*. Physics in Medicine and Biology, 2002. **47**(13): p. 2203-2220.
22. Hodge, W., et al., *Feasibility report of image guided stereotactic body radiotherapy (IG-SBRT) with tomotherapy for early stage medically inoperable lung cancer using extreme hypofractionation*. Acta Oncologica, 2006. **45**(7): p. 890-896.
23. Maryanski, M.J., et al., *Magnetic resonance imaging of radiation dose distributions using a polymer-gel dosimeter*. Physics In Medicine And Biology, 1994. **39**(9): p. 1437-1455.
24. Vandecasteele, J. and Y. De Deene, *On the validity of 3D polymer gel dosimetry: II. Physico-chemical effects*. Physics in Medicine & Biology, 2013. **58**(1): p. 43-61.